CONCEPTUAL DESIGN OPTIMIZATION OF A BLENDED WING BODY (BWB) AIRCRAFT USING FLYING AND HANDLING QUALITIES ASSESSMENT

Clayton HUMPHREYS-JENNINGS[1], Ilias LAPPAS (https://orcid.org/0000-0003-3750-6825)[1], Dragos Mihai SOVAR[1]

[1]*Department of Mechanical and Aeronautical Engineering, Faculty of Computing, Engineering and Science, University of South Wales, Treforest Campus, United Kingdom*

Corresponding author: Ilias Lappas, ilias.lappas@southwales.ac.uk

Abstract. The Blended Wing Body (BWB) configuration is considered to have the potential of providing significant advantages when compared to conventional aircraft designs. At the same time, numerous studies have reported that technical challenges exist in many areas of its design, including stability and control. This study aims to create a novel BWB design to test its flying and handling qualities using an engineering flight simulator and as such, to identify potential design solutions which will enhance its controllability and manoeuvrability characteristics. This aircraft is aimed toward the commercial sector with a range of 3,000 nautical miles, carrying a payload of 20,000kg. In the engineering flight simulator a flight test was undertaken; first, to determine the BWB design's static stability through a standard commercial mission profile, and then to determine its dynamic stability characteristics through standard dynamic modes. Its flying qualities suggested its stability with a static margin of 8.652% of the Mean Aerodynamic Chord (MAC) and consistent response from the pilot input. In addition, the aircraft achieved a maximum lift-to-drag ratio of 28.1; a maximum range of 4,581 nautical miles; zero-lift drag of 0.005; and meeting all the requirements of the dynamic modes.

Keywords: Blended Wing Body (BWB), aircraft conceptual design, engineering flight simulator, flying and handling qualities, aircraft stability.

Introduction

The Blended Wing Body (BWB) aircraft is a non-conventional design in which the fuselage and the wings are combined into one fluid shape instead of three distinct parts assembled. This has the potential of providing various advantages "including a 15% reduction in take-off weight and a 27% reduction in fuel burn per seat mile" (Liebeck, 2004). The reduction in fuel comes from the 15% increase in lift-to-drag ratio meaning less work needs to be done to overcome the effects of drag, but also, the design itself significantly reduces the amount of zero-lift, or parasite, drag that the aircraft is affected by.

This design follows very similar characteristics to that of the 'flying wing', including the downside that, without a horizontal stabiliser, the aircraft is liable to longitudinal instability, which is a phenomenon that has been reported for various prototypes and studies (Okonkwo and Smith, 2016). Apart from the potential flying and handling qualities issues, the BWB concept is also challenged with regards to its weight efficiency (Dubovikov et al, 2019). In theory, flying wings can be designed to be inherently stable (Karl and Wohlfahrt, 1994) and there have been 'flying wings' that have flown successfully; an example of this being the Northrop YB-49. To be able to study the unique performance and stability characteristics of the BWB and the associated technical challenges from a flying and handling qualities point of view, a conceptual BWB design has been created that offers similar performance to a standard commercial aircraft design.

1. Previous Research Efforts

There are currently many research programs that have developed suitable design outcomes on paper; however, these have not been tested on a large scale, simulator, or at all. Those efforts have been supported by NASA, Boeing and multiple universities across Europe and USA and each of these initiatives have provided promising results with suggestions for future research to improve upon which will be inferred throughout the present study.

The Multidisciplinary Optimization of a BWB (MOB) was a joint European venture which has incorporated 15 different universities with the intent to create a Computation Design Engine (CDE) following both a low- and high-fidelity multidisciplinary design process directed at a BWB design with their key objective to "create a system allowing both co-operative and innovative design to be undertaken by a distributed design team employing their own specific design tools and methods" (Morris et al, 2004). Although their focus was more on developing a system that can be used to effectively optimize an array of unique and innovative designs for aircraft, the results from the testing of the CDE yielded interesting results that have been implemented into the present design such as "controllability can be improved by shortening the fuselage" and "increasing the aft-camber of the fuselage profiles". The aerodynamic considerations of the MOB platform have also been studied (Qin et al. 2004).

Liebeck (2004) focused on exploiting the size and efficiency potential of the BWB aircraft opting to create a design for 800 passengers and 7000 nautical mile range in a double decker, double aisle design. The proposed design was compared to a conventional aircraft with the same capabilities utilising multidisciplinary design optimisation. His results were achieved through computational testing using standard equations which demonstrated a "15% reduction in take-off weight and a 27% reduction in fuel burn per seat mile", as well as the BWB being "readily adaptable to cruise Mach numbers as high as 0.95." This comes at very little extra cost in terms of manufacturing with many advantageous opportunities relating to environmental efficiency. Finally, the estimated maximum lift-to-drag ratio (L/D) ratio at cruise is 23 at a great reduction in thrust requirements, using only three engines at 61,600lbsf as compared to a standard design achieving a maximum L/D of 19 and requiring four 63,600lbsf engines.

Work of Van Dommelen and Vos (2014) has attempted to create a systematic algorithm that will enable multidisciplinary optimisation, to which they have ultimately investigated three different and unique design prospects explicitly for the BWB. These three design options are two backward swept wing designs with the engines first mounted under the wing, and then at the trailing edge of the fuselage; and one forward swept wing also with engines under-the-wing mounted. Their results were inconclusive in which is best of the three with each demonstrating solutions to each problem: the forward swept wings meant that the static margin was greatly improved and even had the best ferry range; the forward sweep with under-the-wing engines had the least travelled static margin from take-off to cruise which is crucial for stability overall and had maximum lift coefficient; whilst the forward swept aft-mounted engines had the least fuel consumption and highest maximum L/D at 27.9. Another advantage of aft-mounted engines is that of reduced noise pollution which has become an increasingly important goal of city-based airports.

The X-48B Low Speed Vehicle (LSV) is an 8.5%-scale aircraft of a potential, full-scale BWB type aircraft and is flown remotely from a ground control station using a computerized flight control system located onboard the aircraft, which had the main purpose of looking into the stability of the BWB aircraft (Risch et al, 2009). 39 flights were performed in various configurations which clocked just under 22 hours of flight time, all with positive feedback from the pilot. The most important outcome of this work is that the BWB can be controlled by a pilot without inducing errors and that the design has been flight tested to meet a standard commercial flight envelope as well as further expansion of what the aircraft can handle.

2. Methodology

2.1. Geometry

2.1.1. Weights

Following a relevant market research (Boeing, 2017) (Airbus, 2017), it has been determined that the best region to operate the BWB aircraft of the present study would be the Asia-Pacific region. The design is set to achieve a range of 3,000 nautical miles and to carry a payload weight of 20,000 Kg or 200 people plus baggage, which led to weight estimations using Raymer's (2012) approximations for the initial weights. These were then refined once again after the basic geometry was established and then iterated to convergence, leading to the final weight estimate defined in Table 1.

Table 1. Final Weight Estimate

Type	Weight, Kg	Weight Ratio	Boeing 737-800 Weight, Kg	Boeing 737-800 Weight Ratio	Percentage Difference
Empty Weight	39 523	0.491	41 871	0.517	+ 5.94 %
Fuel Weight	20 869	0.259	21 014	0.259 (max fuel)	+0.69 %
Payload	20 000	0.250	18 170	0.224	- 9.15 %
Gross Weight	80 392	1.000	81 055	1.000	+0.82 %

2.1.2. Wings

Once the weights were determined, the wing geometry was able to be defined; this was calculated for the main wing section only using the Boeing 787-800's aspect ratio of 9.48 (Science Direct, 2019). In addition, the sweep of the aircraft was determined to be 40 degrees. This was chosen since it provides the highest lift-to-drag ratio for a slight negative moment generated at the wings (Siouris and Qin, 2007), (Dababneh et al, 2018). The tendency of the BWB aircraft is to pitch up due to the position of the aerodynamic centre typically being in front of the centre of gravity, and no horizontal stabiliser or tail to counteract it (McParlin et al, 2006). This can be counteracted using mass positioning but also negative moments. Having taken into account all those considerations, Table 2 outlines the results for the wing geometry.

Preprints (www.preprints.org) | NOT PEER-REVIEWED | Posted: 24 November 2019 doi:10.20944/preprints201911.0284.v1

Peer-reviewed version available at Aerospace 2020, 7; doi:10.3390/aerospace7050051

Table 2. Wing Geometry

Type	Value
Span, b	36.81 m
Area, S	142.94 m^2
Taper Ratio, λ	0.225
Root Chord Length, c_{root}	6.34 m
Tip Chord Length, c_{tip}	1.43 m
Mean Aerodynamic Chord (MAC), $\bar{c}$	4.40 m
MAC Distance from centre line, $\bar{Y}$	7.26 m

2.2. Shape Optimisation

2.2.1. XFLR5 (v6.47) Initial Design and Aerofoil Selection

The chosen aerofoil for the inner wing and fin was NACA sc0012 as this proved most stable for the aircraft compared to an asymmetrical aerofoil like the NACA sc2412. However, that aerofoil was used for the outer wing based on its efficiency and that it has the same thickness-to-chord ratio as the inner wing. From the data created by XFLR5 (v6.47), shown in Figure 1, it is seen that the aircraft is stable straight off with a negative gradient for the moment coefficient c_m. Through XFLR5 (v.6.47), the neutral point was determined to be at 13.41 m from the nose, and centre of gravity to be at 12.34 m. This meant a static margin of 8.65 % of the MAC, meaning it is stable and above the recommended 5% static margin.

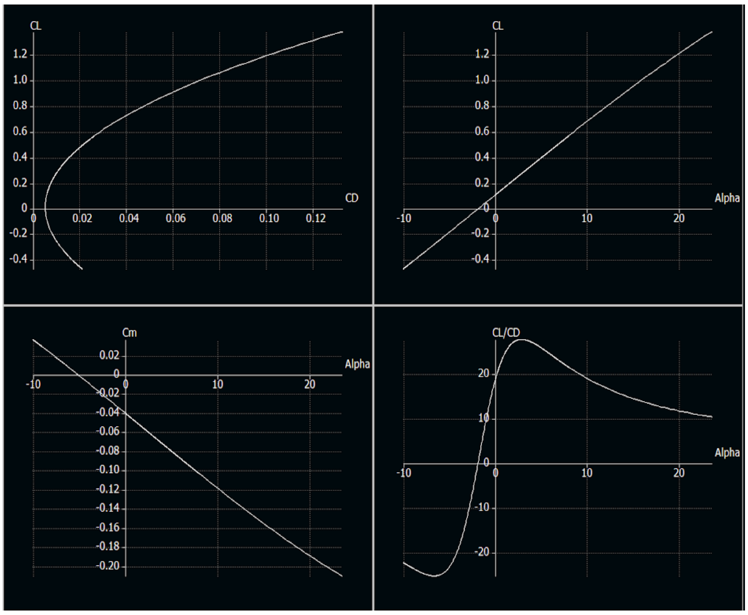

Figure 1. XFLR5 (v6.47) Result Graphs: Top-Left - C_L vs C_D; Top-Right - C_L vs Angle of Attack (α); Bottom-Left - C_m vs α; Bottom-Right - C_L/C_D vs α

2.2.2. Spanwise Lift Distribution & Optimisation

Further development of the wing was done to enable a more efficient and optimised design, which had been observed to have also a positive effect to the flying and handling characteristics of the BWB design. As a first step in optimising the geometry, the main approach that has been considered was imprinting the elliptical lift distribution which yields in the lowest induced drag for a given span. (Jones, 1950). To achieve the specified distribution, the overall geometry has been inputted in OpenVSP (v3.17.0), which employs the Vortex Lattice Method (VLM) with 2nd order Karman-Tsien Mach correction in the aerodynamic analysis module. The methodology implies the variance of four different twist values at different spanwise positions. Figure 2 shows the initial and optimised distributions of the lift for cruise flight conditions, while Figure 3 shows the twist values along the wing. Comparatively, Qin et al. (2005), has determined using a RANS low fidelity optimisation that a twisted wing with a mix of triangular and elliptical distribution is best for the aerodynamics as a compromise between least wave drag with the triangular but the lowest induced drag with respect to the elliptical distribution.

Preprints (www.preprints.org) | NOT PEER-REVIEWED | Posted: 24 November 2019 doi:10.20944/preprints201911.0284.v1

Peer-reviewed version available at Aerospace 2020, 7; doi:10.3390/aerospace7050051

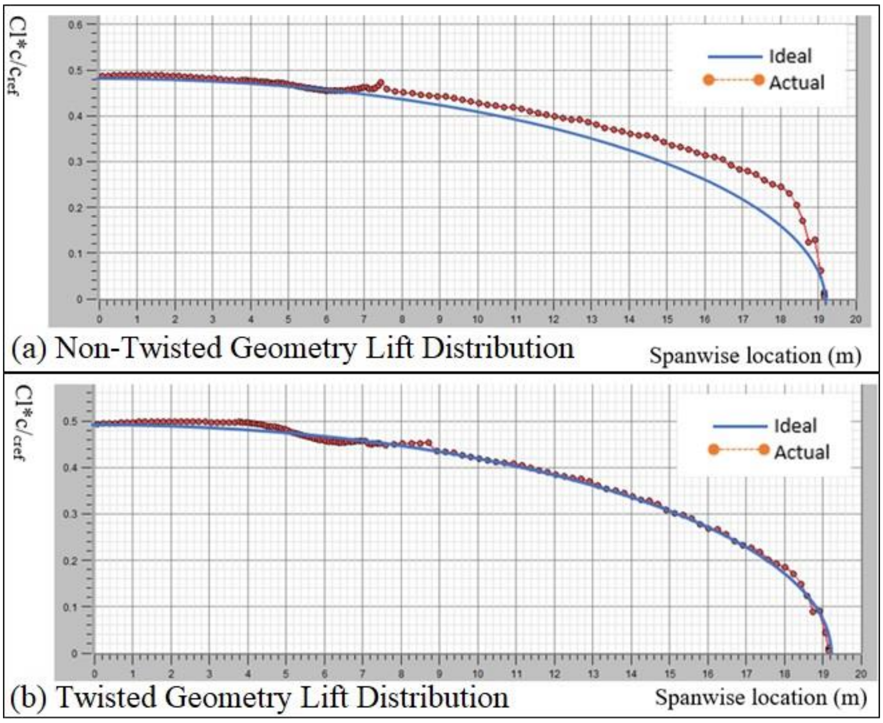

Figure 2. Spanwise lift distribution at cruise flight conditions.

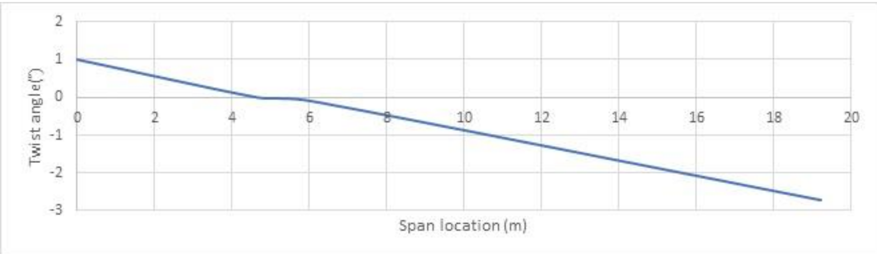

Figure 3. Spanwise twist distribution of the optimised model.

The resulting drag coefficient reduction is presented at the Table 3.

Table 3. Drag coefficient reduction after optimisation

	Induced drag coefficient (C_{DI})	Zero lift drag coefficient (C_{D0})	$C_{D(tot)}$
Non-Twisted	0.0089	0.0046	0.0135
Optimised	0.0086	0.0045	0.0131
Difference	-3.49%	-2.81%	-3.26%

The sectional lift coefficient required for the elliptical lift distribution follows a steadily increasing trend from the middle section plane until the beginning of the wing, as shown in Figure 4. A more visible increment is noticed from the beginning of the wing until a maximum is reached at approximately its middle section. Then, an enhanced decrease is noticed until the beginning of the winglets.

Preprints (www.preprints.org) | NOT PEER-REVIEWED | Posted: 24 November 2019 doi:10.20944/preprints201911.0284.v1

Peer-reviewed version available at Aerospace 2020, 7; doi:10.3390/aerospace7050051

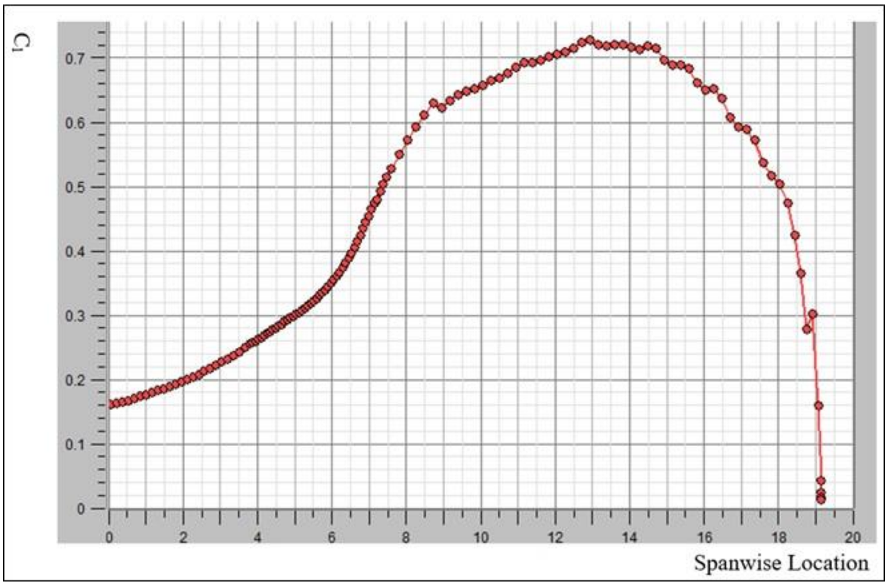

Figure 4. Local Lift Coefficient Distribution over the Spanwise Direction

Kumar & Khalid (2017) have used the same trend of the sectional lift coefficient for a similar BWB concept. However, the method used in the present study for obtaining the twist angles is based on the lift curves. Qin et al. (2002) have employed RANS approach in optimising a BWB concept, which resulted in the same trend obtained for the local lift coefficient distribution when aiming for the elliptical lift distribution. Various views of the optimised shaped configuration are shown at Figure 5.

Preprints (www.preprints.org) | NOT PEER-REVIEWED | Posted: 24 November 2019 doi:10.20944/preprints201911.0284.v1

Peer-reviewed version available at *Aerospace* **2020**, *7*; doi:10.3390/aerospace7050051

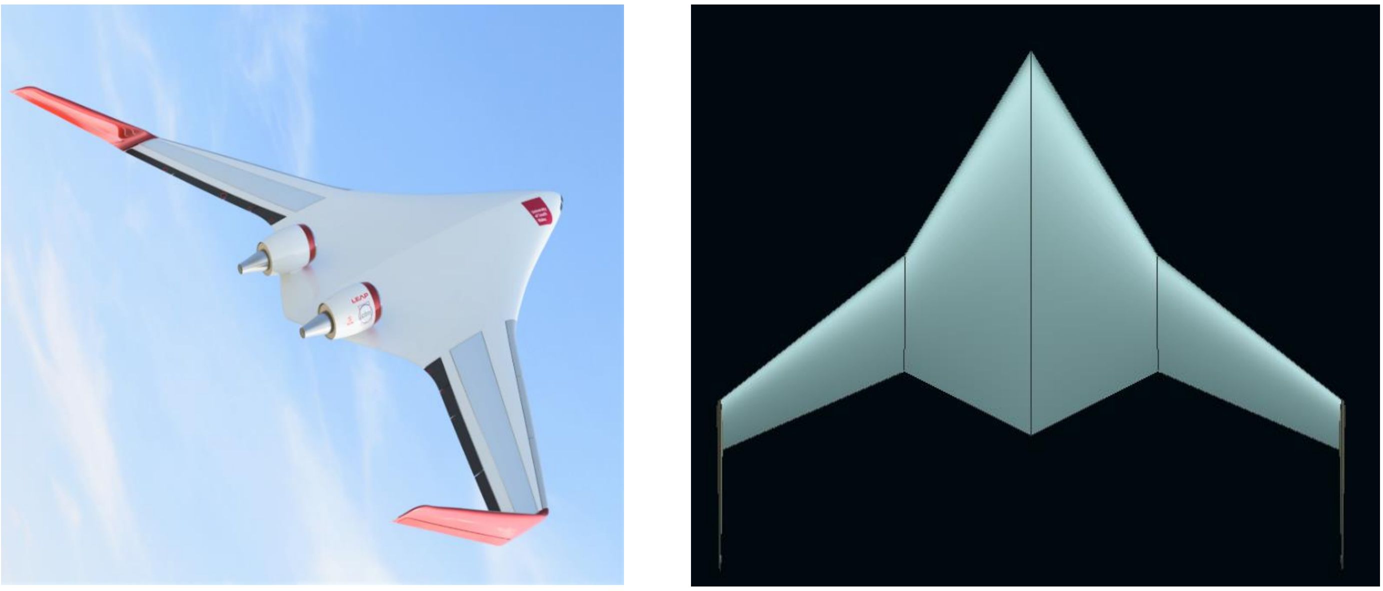

Figure 5. Various Views of the Optimised Shape Configuration

2.3. Design Parameters Overview and Comparison

Below is a table that compares design parameters of the BWB aircraft of the present study (CHJ-BWB) against previously conceptualised design from Van Dommelen and Vos (2014), and of the Boeing 737-800 (van Heerden et al, 2019).

Table 4. Conceptual Comparison

Parameter	CHJ-BWB	van Dommelen and Vos	Boeing 737-800
Wing Area, S, m^2	318.81	1091	124.48
Wing Span, b, m	36.81	64.9	34.32
Aspect Ratio	4.25	3.86	9.45
Wing Loading, N/m^2	2469.22	3650	6158.424
Length, m	30.74	41.40	39.50
MTOW, kg	80,392	406,000	79,002
OEW, kg	39,523	190,000	41,871.06
Payload, kg	20,000	66,400	18,170.46
Fuel Weight, kg	20,869	149,000	21,014.532
Range, nmi	4,581	9,557	4,000
Maximum Lift-to-Drag ratio	28.1	27.9	17.26 (estimated)
Centre of Gravity, % MAC	8.652	14.9	unknown
Take-off Distance, km	3.12	2.00	2.50
Landing Distance, km	1.30	2.48	1.768
Stall Speed (Clean configuration), Knots	130	129	128

3. Simulator Implementation and Flight Testing

Once the BWB design has been finalised, it has been inserted into the Merlin MP521 Engineering Flight Simulator (Merlin Flight Simulation Group, 2019), to test its flying and handling qualities. The MP521 simulator comprises a

Peer-reviewed version available at Aerospace 2020, 7; doi:10.3390/aerospace7050051

capsule with a six axis motion system, visual and instrument displays, touch control panels, and hardware flight controls. The software of the flight simulator that has been run is the Excalibur II, while the design has been created at the Excalibur Data Editor. The model in the editor has utilized the geometrical data and mass properties of the design, in addition to the aerodynamics and propulsion data, acquired during the BWB conceptual design. The mass moments of inertia are calculated by the data editor, using empirical relations, from the inserted values that correspond to the aircraft mass parameters, center of mass and wing span, assuming one plane of symmetry.

The performed simulated flights followed a traditional commercial flight path, and flight testing which included the static and dynamic modes. A secondary objective of the flight test task was to qualify the design to enter the 'IT FLIES UK' aircraft design, flying and handling qualities international competition. This has required specific flight test documents to be written up that helped outline the parameters which had to be monitored when performing the initial flight tests of the aircraft. The rest of the flight tests have focused on meeting the MIL-F-8785C requirements (1980), as it had distinct pass/fail criteria with qualitative values with which to compare against.

MIL-F-8785C (1980) looks at the dynamic modes at the various flight phases. These are divided into three categories, namely A (rapid manoeuvring, e.g. air-to-air combat), B (gradual manoeuvring without precision tracking, e.g. climb and cruise), and C (gradual manoeuvring with precision tracking, e.g. take-off and landing). For the aircraft, it is intended to satisfy both B and C since it will not be performing rapid manoeuvres. Finally, levels of flying quality are labelled from 1 to 3, with 1 being the best, 3 being the worst. This design will be aiming for Level 1 where the aircraft's "Flying qualities clearly adequate for the mission flight phase" because this is meant for commercial aircraft and pilot load is already high without additional input required as in Level 2.

The time to double or half is the time required for the initial perturbation of the trimmed condition to be doubled or halved and is defined at the equation (1),

$$t_{double} \; or \; t_{half} = \frac{ln2}{|n|} = \frac{ln2}{|\zeta|\omega_n} \quad (1)$$

where the symbol n corresponds to the real part of the relevant eigenvalue. The damping ratio ζ is defined by using the equation (2),

$$\zeta = -\frac{n}{\omega_n} \quad (2)$$

n which ω_n is the undamped angular frequency provided by Etkin and Reid (1996) at the equation (3) below.

$$\omega_n = (\omega^2 + n^2)^{0.5} \quad (3),$$

thus, by obtaining the period (T) of the oscillation and the t_{half} or t_{double} after processing the recorded flight data, both damping ratio and the undamped angular frequency can be calculated.

4. Results

4.1. Flying & Handling Qualities

4.1.1. Take off and Initial Climb

The design was able to take-off with Maximum Take Off Weight (MTOW) at 170 knots with flaps at the take-off setting and this required a distance of 2.46 km; the time for which was 46 seconds. The speed for take-off is 1.79 times the stall speed whereas an accepted rule of thumb is that take-off speed be 1.1 times the stall speed, suggesting that the aircraft has more drag in take-off configuration than clean, nearly doubling the amount of speed required before a successful take-off. On testing with a test pilot as part of the 'IT FLIES UK' competition, the pilot has commented that the speed was relatively fast for a take-off and he has suggested if the aircraft can have a slightly more extended take-off flap setting, something which has been incorporated successfully into the final optimised design.

4.1.2. Stall and Landing

The stall speed for the aircraft was recorded at 95 knots with fully extended flaps and 130 knots in clean configuration. Both did not demonstrate a standard nose down stall, but instead displayed nose 'nodding' which was commented on by the test pilot in positive regards. According to Nicolai and Carichner (2010), the approach speed needs to be at least 1.3 times the stall speed, which for our aircraft would be at least 123.5 knots. From the data, it was determined that the average rate of descent for the aircraft in landing configuration was 817 ft/min which was achieved at an average speed of 151 knots indicated airspeed with the pilot commenting that speed control was satisfactory. With the approach speed averaging at 151 knots, this has provided us with a nearly 1.6 times the stall speed safety

Preprints (www.preprints.org) | NOT PEER-REVIEWED | Posted: 24 November 2019 doi:10.20944/preprints201911.0284.v1

Peer-reviewed version available at Aerospace 2020, 7; doi:10.3390/aerospace7050051

margin. Additional testing did indicate that the aircraft would recover on its own if wing drop was induced by the pilot during the stall at various cruising altitudes, but, in general, no wing drop has been observed during a standard stall with wings level. During the landing, pitch control was sensitive with the pilot having no difficulty to fix an appropriate pitch attitude for landing.

4.1.3. Cruise

Cruising conditions were met as part of the specification. The aircraft was able to fly at 35,000ft at 0.85 Mach and performed as expected. The test pilot noted a good overall roll performance and suitable for the mission requirements. During steady cruising conditions, the aircraft did hold its own without any pilot input, which would suggest that static stability is adequate for non-dynamic modes.

4.2. Dynamic Modes Testing

4.2.1. Short Period

The short period can be demonstrated by a sharp and short pull back, or push down, on the control column, releasing it and measure its response in relation to attitude of the aircraft. Through the data it was shown that the time period for the mode was 3.5 seconds meaning a linear frequency of 0.286s $^{-1}$ and an angular frequency of 1.795 rad.s^{-1}. This falls within the expected range of values, which is 1 rad/s to 10 rad/s (Cook, 2013), suggesting that this is an accurate interpretation of the flight simulation data. The calculated value of the damping ratio suggests that the aircraft meets Level 2 safety until load force with respect to alpha (n/α) reaches 1.5. After this it becomes Level 1, with the natural frequency of 2.268rad/s and damping ratio of 0.611. According to MIL-F-8785C (1980), the damping ratio of the short period meets all of the requirements for all the levels of flight.

4.2.2. Phugoid (Long Period)

The phugoid can be initiated by pulling back (or pushing down), on the control column until 10% of the trim speed has been lost (or gained), then releasing it to determine its ability to return to the trimmed condition. Table 5 shows the related phugoid mode results for two different trim airspeeds:

Table 5. Phugoid Comparative Results

Speed (knots)	Sim. Frequency (rad/s)	Theoretical Freq. (rad/s)	% Difference
347	0.0761	0.0776	2.47%
507	0.0558	0.0532	4.77%

The calculated damping ratio came out to be 0.180. In relation to the requirements of MIL-F-8785C (1980), the simulated response meets the requirements set out by the document with its minimum for level 1 flight being a damping ratio of at least 0.04.

4.2.3. Roll Subsidence or Roll mode

Stengel (2004) defines this mode as the "damping effects that normally oppose roll rate"; indicating the forces that are opposing an initiated aircraft roll. For the roll mode, MIL-F-8785C (1980) states that the requirements for category B flying is a roll mode time constant of 1.4s or less, and category C flight to be less than or equal to 1.0s. The maximum roll rate has occurred with -11.53 deg.s^{-1}. The result occurs at 36.8% of the value which is -4.243 deg.s^{-1}. The recorded data showed that this was achieved within 1.25s, which is within the required range. The aircraft even returns above the negative roll rate to bring it back to its datum attitude.

4.2.4. Dutch Roll

The Dutch roll is the oscillation in yaw which is due to the change in velocity at each wing leading to roll (Cook, 2013). The mode is initiated through a quick back-and-forth input of the right and left rudder pedals generating the oscillation. As part of the Dutch roll, the damping ratio for both category B and C phases of flight be greater than or equal to 0.08; while frequency for category B needs to be greater than or equal to 0.4 rad.s^{-1}, but greater than or equal to 1.0 rad.s^{-1} in category C. Natural frequency and damping ratio were calculated to be 2.512 rad.s^{-1} and 0.552 respectively. These values meet the requirements of MIL-F-8785C (1980), suggesting that the mode is satisfactory.

Peer-reviewed version available at Aerospace 2020, 7; doi:10.3390/aerospace7050051

4.2.5. Spiral Mode

During the trials with a slow right rudder that would be released at 20° bank, the BWB aircraft would not go beyond 30°. However, if the pilot was to use the rudder adversely and expeditiously, the aircraft would respond dramatically rolling severely past 20° to 40° in under 2 seconds and continue rolling until it was 90° to the horizon, losing height rapidly. From this, it could be said that with sideslip perturbations, the aircraft would remain stable and safe. However, when an excessive force such as that generated by the pilot in parallel with that of a large crosswind could put the aircraft in risk, particularly when at already low speeds like at the approach and landing phase. A design improvement, which resulted from the analysis of the spiral mode behaviour, was to increase the size of the winglet rudders, a change that has enabled more control and resistance to external interference.

5. Conclusion

The present study suggests that, contrary to the established belief, a BWB design can exhibit desired flying and handling qualities that satisfy typical existing requirements that are applicable to conventional passenger jet configurations. The development of the design included many design improvements and has incorporated feedback that has been based on both test pilot inputs and actual analysis of flight simulation test data of the full size aircraft, in addition to an optimisation study of its lift distribution. As such, a successfully designed and optimised concept for a BWB has been achieved which is statically stable with confirmed dynamic stability flight behaviour. The outcome of the study adds to existing insights about the controllability of a BWB configuration (Voskuijl et al, 2008), (Cook and de Castro, 2004) and reinforces the suggestions of Karl and Wohlfahrt (1994) that a BWB can be designed to be inherently stable.

Acknowledgements

The authors would like to acknowledge Mr Georgios Makris for providing insightful ideas and suggestions.

Funding

The effort received no funding.

Author Contributions

The authors contributed equally to the preparation of the manuscript.

Disclosure Statement

No competing financial, professional, or personal interests exist from other parties.

References

Airbus (2017). *Global Market Forecast - Growing Horizons: 2017/2036*. [online] Available at: http://www.airbus.com/content/dam/corporate-topics/publications/backgrounders/Airbus_Global_Market_Forecast_2017-2036_Growing_Horizons_full_book.pdf

Boeing (2017). *Current Market Outlook: 2017 - 2036*. [online] Available at: http://www.boeing.com/resources/boeingdotcom/commercial/market/current-market-outlook-2017/assets/downloads/2017-cmo-6-19.pdf

Cook, M. V. (2013). Flight Dynamics Principles. A Linear Systems Approach to Aircraft Stability and Control. 3rd ed. Amsterdam, Boston: Butterworth - Heinemann.

Cook, M.V. and de Castro, H.V., (2004). The Longitudinal Flying Qualities of a Blended Wing Body Civil Transport Aircraft. *Aeronautical Journal*, *1080* (108), pp. 75-84.

Dababneh, O., Kipouros, T., Whidborne, J.F., (2018). Application of an Efficient Gradient-Based Optimisation Strategy for Aircraft Wing Structures. *Aerospace*, *5*(1), 3.

Dubovikov, E., Fomin, D., Guseva, N., Kondakov, I., Kruychkov, E., Mareskin, I., Shanygin, A., (2019). Manufacturing Aspects of Creating Low-Curvature Panels for Prospective Civil Aircraft. *Aerospace*, *6*(2), 18.

Etkin, B. and Reid, L.D., (1995). *Dynamics of Flight: Stability and Control.* 3rd ed. New York: Wiley.

Jones, R. T. (1950). The spanwise distribution of lift for minimum induced drag of wings having a given lift and a given bending moment. Technical report TN-2249, NASA Ames Research Center, CA, USA.

Karl, N. and Wohlfahrt, M. (1994). Tailless Aircraft In Theory and Practice. Washington DC, USA: AIAA Education Series.

Kumar, P., & Khalid, A. (2017). Blended Wing Body Propulsion System Design. *International Journal of Aviation, Aeronautics and Aerospace*, *4*(4), 1-43. doi:10.15394/ijaaa.2017.1187

Liebeck, R. (2004). Design of the Blended Wing Body Subsonic Transport. *Journal of Aircraft*, 41(1), pp.10-25.

Merlin Flight Simulator Group, *The Merlin MP521 Engineering Flight Simulator*, Merlin Products Ltd. and Merlin Flight Simulation Technologies, (2019, Oct 3), Retrieved from http://www.merlinsim.com/mp521.htm

Morris, A., Arendsen, P., La Rocca, G., Laban, M., Voss, R. and Hönlinger, H. (2004). *MOB-A European Project on Multidisciplinary Design Optimisation*. In *24th ICAS Congress*. Yokohama, Japan.

McParlin, C., Bruce, R.J., Hepworth, A. G., and Rae, A.J. (2006). *Low Speed Wind Tunnel Tests on the 1303 UCAV concept (AIAA 2006-2985)*. In *24th Applied Aerodynamics Conference*. 5-8 June 2006, San Francisco, California, USA

Nicolai, L. and Carichner, G. (2010). *Fundamentals of Aircraft and Airship Design: Aircraft Design; Volume I*. American Institute of Aeronautics and Astronautics, p.157.

Okonkwo, P. and Smith, H. (2016). Review of Evolving Trends in Blended Wing Body Aircraft Design. *Progress in Aerospace Sciences*, 82, pp.1-23.

Qin, N., Vavalle, A., Moigne, A. L., Laban, M., Hackett, K., & Weinerfelt, P. (2002). Aerodynamic studies for blended wing body aircraft. *9th AIAA/ISSMO Symposium on Multidisciplinary Analysis and Optimization* (pp. 1-11). Atlanta, Georgia, USA: American Institute of Aeronautics and Astronautics, Inc.

Qin, N., Vavalle, A., Le Moigne, A., Laban, M., Hackett, K. and Weinerfelt, P. (2004). Aerodynamic Considerations of Blended Wing Body Aircraft. *Progress in Aerospace Sciences*, *40*, pp.321-343.

Qin, N., Vavalle, A. and Moigne, A.L., (2005). Spanwise Lift Distribution for Blended Wing Body Aircraft. *Journal of aircraft*, *42*(2), pp.356-365.

Raymer, D. (2012). *Aircraft design*. 5th ed. Reston, VA: American Institute of Aeronautics and Astronautics

Risch, T., Cosentino, G., Regan, C., Kisska, M. and Princen, N., 2009, January. X-48B Flight Test Progress Overview. In 47th AIAA Aerospace Sciences Meeting including The New Horizons Forum and Aerospace Exposition (p. 934).

Science Direct Topics, *Boeing 787 Dreamliner-An overview*, Elsevier, (2019, Oct 3), Retrieved from https://www.sciencedirect.com/topics/engineering/boeing-787-dreamliner/pdf

Peer-reviewed version available at *Aerospace* **2020**, *7*; doi:10.3390/aerospace7050051

Siouris, S. and Qin, N. (2007). Study of the effects of wing sweep on the aerodynamic performance of a blended wing body aircraft. *Proceedings of the Institution of Mechanical Engineers, Part G: Journal of Aerospace Engineering*, [online] 221(1), pp.47-55. Available at: http://journals.sagepub.com/doi/pdf/10.1243/09544100JAERO93

Stengel, R. (2004). *Flight dynamics*. Princeton, NJ [u.a.]: Princeton University Press, p.330.

United States Department of Defense. (1980). MIL-F-8785C, Military Specification - Flying Qualities of Piloted Airplanes, Arlington, Virginia, USA.

van Heerden, A.S.J., Guenov, M.D., Molina-Cristobal, A. (2019). Evolvability And Design Reuse in Civil Jet Transport Aircraft. *Progress in Aerospace Sciences*, 108, pp.121-155.

van Dommelen, J. and Vos, R. (2014). Conceptual design and analysis of blended-wing-body aircraft. *Proceedings of the Institution of Mechanical Engineers, Part G: Journal of Aerospace Engineering*, [online] 228(13), pp.2452-2474. Available at: http://journals.sagepub.com/doi/abs/10.1177/0954410013518696

Voskuijl, M., La Rocca, G., and Dircken, F. (2008). *Controllability of Blended Wing Body Aircraft*. In *26th ICAS Congress*. Anchorage, Alaska, USA.